

Quark distributions in the pion

**Dirk Brömmel^{*†a,b}, Markus Diehl^b, Meinulf Göckeler^a, Philipp Hägler^c,
Roger Horsley^d, Yoshifumi Nakamura^e, Dirk Pleiter^e, Paul E.L. Rakow^f,
Andreas Schäfer^a, Gerrit Schierholz^{b,e}, Hinnerk Stüben^g and James M. Zanotti^d**

^a*Institut für Theoretische Physik, Universität Regensburg, 93040 Regensburg, Germany*

^b*Theory Group, Deutsches Elektronen-Synchrotron DESY, 22603 Hamburg, Germany*

^c*Institut für Theoretische Physik T39, Physik-Department der TU München,
85747 Garching, Germany*

^d*School of Physics, University of Edinburgh, Edinburgh EH9 3JH, UK*

^e*John von Neumann-Institut für Computing NIC / DESY, 15738 Zeuthen, Germany*

^f*Theoretical Physics Division, Dep. of Math. Sciences, University of Liverpool,
Liverpool L69 3BX, UK*

^g*Konrad-Zuse-Institut für Informatik ZIB, 14195 Berlin, Germany*

E-mail: dirk.broemmel@desy.de

QCDSF/UKQCD Collaboration

We compute the lowest three non-trivial moments of the quark distribution functions in the pion. We also present results of the generalisation to moments of vector and tensor GPDs that are related to the distribution of quarks in the transverse plane. We find a distortion of the distribution of polarised quarks that is similar to that observed in the nucleon. The simulation is done using two flavours of dynamical fermions with pion masses down to 340 MeV. Important features of our investigation are the use of $\mathcal{O}(a)$ improved Wilson fermions and non-perturbative renormalisation.

*The XXV International Symposium on Lattice Field Theory
July 30 - August 4 2007
Regensburg, Germany*

*Speaker.

†Present address: School of Physics and Astronomy, University of Southampton

1. Introduction

The pion plays an important rôle in nuclear and particle physics. Identified as a pseudo Goldstone boson of chiral symmetry breaking it has a prominent position in the low energy sector of quantum chromodynamics (QCD). Furthermore, with its two valence quarks and spin zero it is one of the most basic bound states in QCD and hence appears to be simple. The internal structure of the pion is, however, not very well known. This has to be seen in connection with the difficult experimental situation. Among the few experimentally measured quantities are the electromagnetic form factor F_π and parton distribution functions (PDFs). The latter quantities are less well known than for the nucleon, with the last experimental results dating back to the late 1980's. One uncertainty of the measured pion PDFs is the unconstrained distribution of sea quarks. The accessible information for the PDFs also relies heavily on input from nucleon PDFs and the knowledge of nuclear effects to correct for scattering on a tungsten target [1], adding additional ambiguities. The second observable highlighted in these proceedings, the distribution of transversely polarised quarks inside the pion, has not been measured experimentally. Clearly, lattice QCD is in the unique position to provide additional or, as in the latter case, first results from first principles.

2. Generalised Parton Distributions

A powerful tool to investigate the structure of hadrons are generalised parton distributions (GPDs). They are defined by non-local matrix elements evaluated on the light cone (see [2] for a definition). GPDs contain both PDFs and the electromagnetic form factor as limiting cases and are a generalisation of these known observables. For the pion two GPDs exist: the vector and tensor GPDs $H_\pi^q(x, \xi, \Delta^2)$ and $E_{T,\pi}^q(x, \xi, \Delta^2)$, respectively. Both depend on three kinematic variables, namely the momentum fraction x of the pion's momentum carried by the struck quark q , the longitudinal momentum fraction $2\xi = -\Delta^+/P^+$, and the momentum transfer $\Delta^\mu = p'^\mu - p^\mu$. Here p^μ and p'^μ are the momenta of the incoming and outgoing pion, and P^μ is their average.

In the forward limit where $\Delta \rightarrow 0$, the momenta of the pion states are equal and the matrix elements take the form used in the definition of PDFs, making the connection to the GPD H_π^q apparent. We arrive at the probability density $q(x)$ of finding a parton q with a given momentum fraction x . We can write

$$H_\pi^q(x, 0, 0) = \Theta(x)q(x) - \Theta(-x)\bar{q}(x), \quad -1 \leq x \leq 1. \quad (2.1)$$

The relation of GPDs to form factors is found when integrating H_π^q over the momentum fraction x . The operator in the matrix element then becomes the local vector current so that we have

$$\int dx H_\pi^u(x, \xi, \Delta^2) = F_\pi(\Delta^2). \quad (2.2)$$

This is the lowest possible Mellin moment for which the integrand is weighted with x^n ($n = 0, 1, 2, \dots$) for the $(n+1)$ -th moment. In general, Mellin moments turn the non-local light cone matrix elements to local ones involving n covariant derivatives. These matrix elements of local operators are the quantities calculated on the lattice. They are parametrised by generalised form

factors (GFFs) $A_{n,i}^\pi$ and $B_{Tn,i}^\pi$ as

$$\langle \pi(p') | \mathcal{S} \bar{u}(0) \gamma^{\mu_1} \overleftrightarrow{D}^{\mu_2} \dots \overleftrightarrow{D}^{\mu_n} u(0) | \pi(p) \rangle = 2\mathcal{S} \sum_{\substack{i=0 \\ \text{even}}}^n \Delta^{\mu_1} \dots \Delta^{\mu_i} P^{\mu_{i+1}} \dots P^{\mu_n} A_{n,i}^\pi(\Delta^2), \quad (2.3)$$

$$\begin{aligned} \langle \pi(p') | \mathcal{A} \mathcal{S} \bar{u}(0) i\sigma^{\mu\nu} \overleftrightarrow{D}^{\mu_1} \dots \overleftrightarrow{D}^{\mu_{n-1}} u(0) | \pi(p) \rangle \\ = \mathcal{A} \mathcal{S} \frac{P^\mu \Delta^\nu - \Delta^\mu P^\nu}{m_\pi} \sum_{\substack{i=0 \\ \text{even}}}^{n-1} \Delta^{\mu_1} \dots \Delta^{\mu_i} P^{\mu_{i+1}} \dots P^{\mu_{n-1}} B_{Tn,i}^\pi(\Delta^2), \end{aligned} \quad (2.4)$$

where we first symmetrise (\mathcal{S}) in μ_1, \dots, μ_n or ν, μ_1, \dots, μ_n , then anti-symmetrise (\mathcal{A}) in μ, ν and finally subtract the traces. Here we consider up-quarks for definiteness. Comparing (2.2) and (2.3) we see that $A_{10}^\pi = F_\pi$. Knowledge of all GFFs would be equivalent to knowing the GPDs. However, in practice only the lowest few moments can be calculated. Considering the forward limit again, we find for the Mellin moments of the vector GPD

$$\langle x^n \rangle = \int dx x^n H_\pi^u(x, 0, 0) = \int_0^1 dx x^n [u(x) - (-1)^n \bar{u}(x)], \text{ for } n = 0, 1, 2, \dots \quad (2.5)$$

The moments thus involve the sum or the difference of quark and anti-quark distributions for odd and even n .

3. Results

Our simulation was done using $\mathcal{O}(a)$ improved Clover Wilson fermions with two dynamical flavours and Wilson glue. The set of lattices comprises four β values with three to six κ values each, which have been generated within the QCDSF, UKQCD and DIK collaborations. The pion masses reach down to about 350 MeV with a lattice spacing a between 0.07 fm and 0.12 fm. Our lattice sizes are $16^3 \times 32$, $24^3 \times 48$, and $32^3 \times 64$ with physical spatial size of up to 2.5 fm, where we use the Sommer parameter with $r_0 = 0.467$ fm to set the physical scale. Furthermore we use non-perturbative renormalisation to obtain results in the $\overline{\text{MS}}$ scheme at a scale $\mu = 2$ GeV [3].

The techniques for calculating and extracting the necessary three-point functions have been explained in earlier publications [4, 5, 6].

3.1 Moments of Parton Distributions

We use operators named \mathcal{O}_{v2b} , \mathcal{O}_{v3} , and \mathcal{O}_{v4} with up to three derivatives (see, e.g., [4, 7]) to obtain the moments $\langle x^n \rangle$ with $n = 1, 2, 3$. The preliminary results for our different lattices are shown in Fig. 1. Here we have considered \mathcal{O}_{v2b} for vanishing pion momentum, while the other two operators require one unit of momentum. The statistical errors for $\langle x \rangle$ are thus considerably smaller. Also included in the plot is an extrapolation linear in the square of the pion mass. Note that one-loop chiral perturbation theory predicts such a linear relation only for $\langle x^n \rangle$ with odd n [2]. In order to reach firm conclusions one has to take into account the systematic uncertainties. These will be discussed in detail in an upcoming paper. The effects due to the limited physical volume are most prominent. To get an idea about the size of these effects, we include a simple volume dependent term in our extrapolation

$$\langle x^n \rangle(m_\pi, L) = c_0 + c_1 m_\pi^2 + c_2 m_\pi^2 e^{-m_\pi L}, \quad (3.1)$$

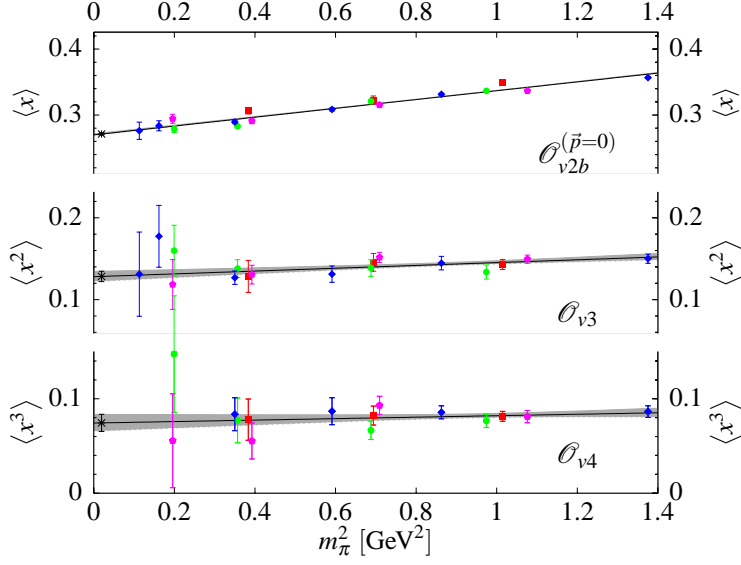


Figure 1: The moments $\langle x^n \rangle$ extrapolated linearly in the square of the pion mass. The coding of the symbols is according to the β values: (red) squares, (green) circles, (blue) diamonds, and (purple) hexagons for $\beta = 5.20, 5.25, 5.29, 5.40$, respectively. The solid line and error band show a linear fit in m_π^2 , the star represents the extrapolated value at the physical pion mass.

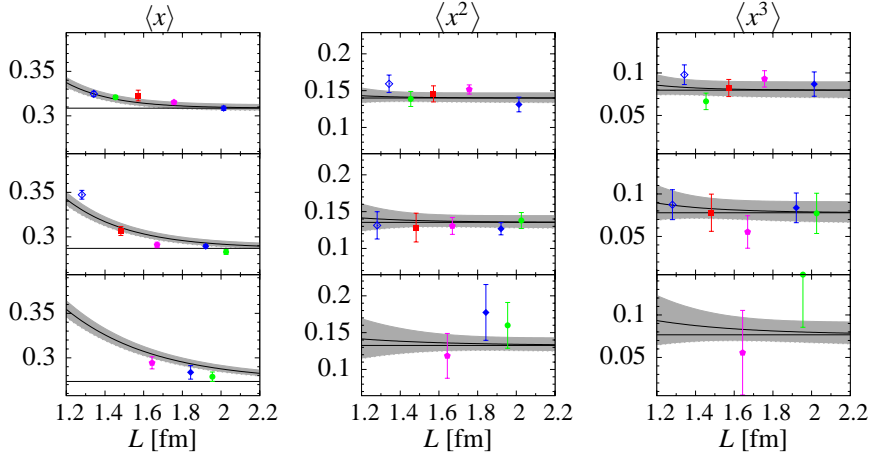


Figure 2: Estimates of the finite size effects for the moments $\langle x^n \rangle$. The panels are for $n = 1, 2, 3$ from left to right and pion masses around 800 MeV, 600 MeV, and 430 MeV from top to bottom. The open symbols refer to our finite size runs and the fit and its error band are for the corresponding average pion mass. Colour/symbol coding as before.

where L is the lattice size. A combined fit to our lattice data profits from two additional finite size runs where only the physical volume has been varied. The results of such fits are shown in Fig. 2, displaying groups of our lattice data of similar pion mass (800 MeV, 600 MeV and 430 MeV). Because of the size of our statistical errors, only the lowest moment $\langle x \rangle$ shows a clear dependence on the volume and we expect our results to decrease in the infinite volume. Note that our lowest pion masses are affected more drastically. We estimate a finite size effect of the order of 10% for the smallest pion masses.

We compare our results to two different PDF parametrisations extracted from experiment.

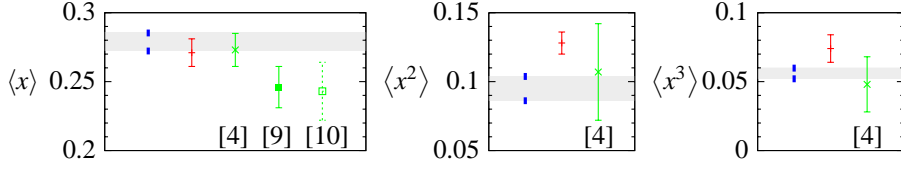


Figure 3: Comparison of phenomenological and lattice data. The upper value of the band is calculated from [1] while the lower one is the value from [8]. The (red) plus is the current data and we include lattice data from the other references as labelled in the plot. The scale is always taken to be $\mu = 2 \text{ GeV}$ apart from [4] which is for $\mu \approx 2.4 \text{ GeV}$.

The first one uses a parametrisation of similar form as in the nucleon case [1], the other one uses a constituent quark model closely related to the proton PDFs [8]. This comparison is shown in Fig. 3, which also includes other lattice data from quenched simulations [4, 9, 10]. The number from [10] is a result close the physical pion mass and no extrapolation has been taken. It is important to note that our lattice results for $\langle x^n \rangle$ lack contributions from disconnected fermion lines when $n = 1$ or 3. The preliminary numbers for the moments of the quark PDF in $\overline{\text{MS}}$ at $\mu = 2 \text{ GeV}$ are $\langle x \rangle = 0.271(2)(10)$, $\langle x^2 \rangle = 0.128(6)(5)$ and $\langle x^3 \rangle = 0.074(9)(4)$, with quoted uncertainties only from statistical and renormalisation errors.

3.2 Transverse Spin Structure

The second observable covered in these proceedings is the distribution of transversely polarised quarks inside the pion. We will only focus on the basic idea, more details can be found in [11]. Starting point is an operator that projects out quarks with transverse polarisation \vec{s} : $\frac{1}{2}\bar{q}[\gamma^+ - s^j i\sigma^{+j}\gamma_5]q$, [12]. It is connected to the GPDs $H_\pi^q(x, \xi, \Delta^2)$ and $E_{T,\pi}^q(x, \xi, \Delta^2)$ when measured between pion states. A Fourier transform with respect to Δ_\perp for $\xi = 0$ makes a probabilistic interpretation possible, leading to densities $\rho(x, \vec{b}_\perp)$ in the transverse plane [13]:

$$\rho^u(x, \vec{b}_\perp) = \frac{1}{2} \left(H_\pi^u(x, \vec{b}_\perp^2) - \frac{s^i \epsilon^{ij} b_\perp^j}{m_\pi} \frac{\partial}{\partial \vec{b}_\perp^2} E_{T,\pi}^u(x, \vec{b}_\perp^2) \right). \quad (3.2)$$

Here the Fourier transformed GPDs appear and we have again used up-quarks. The important point to note is the correlation between the transverse position \vec{b}_\perp of the quark and its spin \vec{s} . Depending on the size of $E_{T,\pi}^u$ we will thus find a deformation of the distribution of quarks.

Our lattice calculation can again only provide moments of this density which are given in terms of the Fourier transformed GFFs $A_{n,i}^\pi(\Delta^2)$ and $B_{T,n,i}^\pi(\Delta^2)$ from Eqs. (2.3) and (2.4). The lowest moment of the density $\rho^u(x, \vec{b}_\perp)$ needs the two GFFs $A_{1,0}^\pi$ and $B_{T,1,0}^\pi$. In order to perform the Fourier transform, we need to parametrise our data as follows:

$$F(\Delta^2) = F(0) \left(1 - \frac{\Delta^2}{pM^2} \right)^{-p}, \quad (3.3)$$

where F can be any of our GFFs. Our lattice data does not constrain the exponent p very strongly. However, requiring that the density ρ^u is regular at the origin, it follows that $p > 1$ for $A_{n,0}^\pi$ and $p > 3/2$ for $B_{T,n,0}^\pi$ [12].

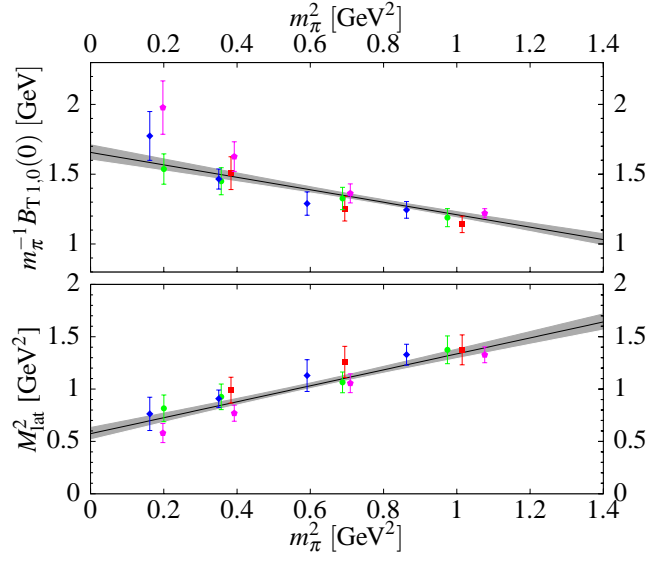


Figure 4: Linear extrapolation of $B_{T1,0}^\pi/m_\pi$ and M^2 against m_π^2 . The colour/symbol coding is the same as in Fig. 1.

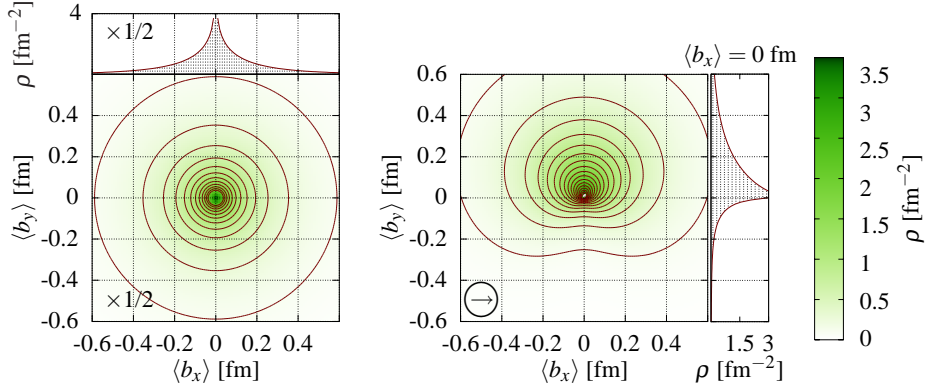


Figure 5: The lowest moment of the quark distribution in the transverse plane. The l.h.s. shows the unpolarised case obtained from $A_{1,0}^\pi(\vec{b}_\perp^2)$, the r.h.s. is for transversely polarised up-quarks inside the pion. The orientation of the spin is as indicated in the plot.

The data for $A_{1,0}^\pi$ is taken from [6] using a pole-fit with $p = 1.1$. The data for $B_{T1,0}^\pi$ is fitted with an exponent $p = 1.6$. The corresponding results for $m_\pi^{-1}B_{T1,0}^\pi(0)$ and the pole mass are shown in Fig. 4. This figure also includes extrapolations linear in the squared pion mass. The extrapolation of $B_{T1,0}^\pi(0)$ is guided by chiral perturbation theory, which finds that $B_{T1,0}^\pi(0)$ should vanish as the pion mass goes to zero [2]. The fits give $m_\pi^{-1}B_{T1,0}^\pi(0) = 1.648(54)$ and $M = 0.767(40)$ GeV at the physical pion mass. The slight change of the results compared to [11] are due to a different choice in fit ranges. Note that the errors are statistical only, see [11] for the influence of lattice artefacts.

The resulting density $\rho^q(x, \vec{b}_\perp)$ is shown in Fig. 5 and exhibits a very clear correlation of quark spin and transverse position.

4. Acknowledgements

The numerical calculations have been performed on the Hitachi SR8000 at LRZ (Munich), APEmille and apeNEXT at NIC/DESY (Zeuthen) and BlueGene/Ls at NIC/FZJ (Jülich), EPCC (Edinburgh) and KEK (by the Kanazawa group as part of the DIK research program). This work was supported by the DFG (Forschergruppe Gitter-Hadronen-Phänomenologie and Emmy-Noether program), by HGF (contract no. VH-NG-004) and by EU I3HP (contract no. RII3-CT-2004-506078).

References

- [1] P. J. Sutton *et al.*, *Parton distributions for the pion extracted from Drell-Yan and prompt photon experiments*, *Phys. Rev.* **D45** (1992) 2349.
- [2] M. Diehl, A. Manashov, and A. Schäfer, *Generalized parton distributions for the pion in chiral perturbation theory*, *Phys. Lett.* **B622** (2005) 69 [hep-ph/0505269]; M. Diehl, A. Manashov, and A. Schäfer, *Generalized parton distributions for the nucleon in chiral perturbation theory*, *Eur. Phys. J.* **A31** (2007) 335 [hep-ph/0611101].
- [3] Paper in preparation.
- [4] C. Best *et al.*, *Pion and rho structure functions from lattice QCD*, *Phys. Rev.* **D56** (1997) 2743 [hep-lat/9703014].
- [5] **QCDSF/UKQCD** Collaboration, D. Brömmel *et al.*, *Structure of the pion from full lattice QCD*, *PoS LAT2005* (2005) 360 [hep-lat/0509133].
- [6] **QCDSF/UKQCD** Collaboration, D. Brömmel *et al.*, *The pion form factor from lattice QCD with two dynamical flavours*, *Eur. Phys. J.* **C51** (2007) 335 [hep-lat/0608021].
- [7] **QCDSF** Collaboration, M. Göckeler *et al.*, *A lattice determination of moments of unpolarised nucleon structure functions using improved wilson fermions*, *Phys. Rev.* **D71** (2005) 114511 [hep-ph/0410187].
- [8] M. Glück, E. Reya, and I. Schienbein, *Pionic parton distributions revisited*, *Eur. Phys. J.* **C10** (1999) 313 [hep-ph/9903288].
- [9] **Zeuthen-Rome (ZeRo)** Collaboration, M. Guagnelli *et al.*, *Non-perturbative pion matrix element of a twist-2 operator from the lattice*, *Eur. Phys. J.* **C40** (2005) 69 [hep-lat/0405027].
- [10] S. Capitani *et al.*, *Parton distribution functions with twisted mass fermions*, *Phys. Lett.* **B639** (2006) 520 [hep-lat/0511013].
- [11] **QCDSF/UKQCD** Collaboration, D. Brömmel *et al.*, *The spin structure of the pion*, arXiv:0708.2249 [hep-lat].
- [12] M. Diehl and P. Hägler, *Spin densities in the transverse plane and generalized transversity distributions*, *Eur. Phys. J.* **C44** (2005) 87 [hep-ph/0504175].
- [13] M. Burkardt, *Impact parameter space interpretation for generalized parton distributions*, *Int. J. Mod. Phys.* **A18** (2003) 173 [hep-ph/0207047].